Journal of Sound and Vibration (2002) **258**(5), 867–883
doi:10.1006/jsvi.2002.5186, available online at http://www.idealibrary.com on IDEAL®

VOLUME VELOCITY ESTIMATION WITH ACCELEROMETER ARRAYS FOR ACTIVE STRUCTURAL ACOUSTIC CONTROL

T. C. Sors†

Industrial Research Limited (IRL), Brooke House, 24 Balfour Road, PO Box 2225, Auckland, New Zealand. E-mail : t.sors@irl.cri.nz

AND

S. J. Elliott

Institute of Sound and Vibration Research (ISVR), University of Southampton, Highfield, Southampton SO17 1BJ, England

(*Received* 1 *March* 2001, *and in final form* 15 *March* 2002)

Controlling the volume velocity of a plate has previously been shown to be a good strategy to reduce its overall sound radiation. Although distributed volume velocity sensors have been developed they have some inherent limitations, particularly the fact that they cannot measure whole-body motion which can have large volumetric components. In this paper, a number of accelerometers are placed on the plate and their outputs are summed in order to estimate the volume velocity. It is found that, by increasing the number of evenly spaced accelerometers, improved estimates of the true volume velocity can be obtained. The number of accelerometers required for a good estimate of volume velocity is also calculated analytically and this value is found to agree with the value found from the simulations. Some further cost functions using accelerometers are also outlined, such as controlling the frequency-dependent shape of the first radiation mode although the results are not very much better then controlling the sum of their outputs. The use of arrays of accelerometers hold some promise for future practical applications of active control as their performance continues to improve and their prices decrease.

1. INTRODUCTION

Active structural acoustic control (ASAC) is a branch of active control in which structural actuators are used to reduce sound radiation from plates instead of using actuators in the acoustic field as is the case in conventional active sound control (ASC). ASAC also differs from active vibration control (AVC) in that it attempts to control only the vibrations which are important to sound radiation or which radiate sound efficiently. Conventional vibration control on the other hand attempts to reduce the vibrations of a structure as much as possible with no concern for the resulting sound radiated by the structure. This results in situations where even though the vibrational levels of a structure are decreased, the overall sound radiation can actually be increased. Conversely, reduction in sound radiation can be achieved even with an increase in a structure's vibrational levels.

† At ISVR while this work was completed.

0022-460X/02/$35.00

The first references to ASAC appeared around 1990 and used point forces to control structural modes of a plate, whilst examining the effects on the radiated sound power [1–3]. More recently, piezoceramic actuators have been used instead of point forces as they have a number of practical advantages such as the fact that they do not require reaction mounts [4–6]. A good overview of ASAC is given in reference [7].

As well as using structural actuators, it is now common to integrate sensors with the structure to be controlled rather than using microphones in the far field to measure the radiated sound. A major advantage when both actuators and sensors are integrated is that the system can be used when it would be impractical to have transducers placed in the acoustic far field. Recent developments of piezoelectric materials have enabled new sensors to be designed. Many of these focus on the use of PVDF film which can be shaped easily to target the control of individual modes. Where structural sensors are used, they must measure variables which are strongly related to the radiated sound power. The use of structural sensors is reviewed in references [7, 8].

As well as developments in transducer technology, another important development in the field of ASAC has been research into the most efficient methods of controlling structural vibrations such that the radiated sound power is reduced. These control strategies have led to the development of the radiation mode approach [9] which is used in this paper, and more elaborate methods of trying to predict the radiated sound power using structurally measured variables measured at a number of points [10].

Radiation modes are sets of independently radiating velocity distributions and, although a number of authors developed similar methods of analyzing them at around the same time, the techniques used in this paper were introduced in references [9, 11, l2]. The third of these references also gives a comparison of the different radiation mode approaches.

At low frequencies, the first radiation mode accounts for most of the sound radiation and has a shape corresponding to the volume velocity of the panel. The sound radiation from the panel could thus be significantly reduced by the control of a single structural variable. This led to the development of volume-velocity sensors which consisted of etching quadratic strips into PVDF film [9, 13]. An example of the use of these volume velocity sensors in experiments is described in reference [14].

One disadvantage of the PVDF volume velocity sensors is that they are essentially strain sensors and so are unable to measure whole-body motion, which can give rise to significant volumetric vibrations. The main purpose of this paper is to investigate whether a number of accelerometers, with their outputs summed, can be used to obtain an approximation to the volume velocity. A similar use of accelerometers is suggested in references [15–18], where it is used to obtain the radiated power in a single direction. Multiple piezoelectric patch sensors have also been used instead of accelerometers in a method similar to the one outlined below [19].

The paper is divided into four further sections. In the first, the theory of radiation modes is briefly reviewed and the reasons for looking to control volume velocity are examined. Section 3 compares using the summed output from an increasing number of accelerometers as an error signal with the control of true volume velocity. This comparison is in terms of the control performance measured by the power radiated by the plate. Section 4 considers other multi-channel cost functions which could be used, where the outputs of the accelerometers are manipulated in some other way rather than by a simple summation. These further control strategies all take into account further properties of the radiation modes, but in doing so increase the complexity of the controller.

2. VOLUME VELOCITY

An important consideration in ASAC is which structural quantities should be measured in order to give a signal which is strongly related to the sound power. In this paper, this is achieved through the use of radiation modes and their theory is reviewed in this section.

Radiation modes, which are a set of independently radiating velocity distributions, are described in detail by Johnson and Elliott [11, 12], but there are two important properties outlined here which are important for ASAC purposes; the efficiency and shape of the first radiation mode.

The motivation for using radiation modes is that although the structural modes, which are normally used to analyze plate vibrations, form a set of orthogonal mode shapes, they do not radiate sound independently. The sound radiated by any one structural mode is dependent on the amplitude and phase of every other structural mode. Apart from at the resonant frequency of one of these modes, the effect of reducing the mode's amplitude on the overall sound radiation cannot be easily predicted. It would thus make sense to develop a method of analyzing plate vibrations in terms of patterns which do radiate sound independently and these are termed radiation modes. There are a number of different mathematical formulations for analyzing radiation modes [12], but they all have the property that they radiate sound independently. In contrast to the control of structural modes, it is clear that by reducing the amplitude of any radiation mode, the total sound radiated by a structure is sure to be reduced.

In this paper, an approach is used in which the vibration of the plate is approximated by dividing the surface into a large number, I, of elemental sources which are small compared with the acoustic wavelength and which oscillate harmonically. The power radiated, W_{el}, by a single element el is given by the element's complex velocity, v_{el}, and the complex pressure, p_{el}, at the elemental position

$$W_{el} = \left(\frac{S_{el}}{2}\right)\Re(v_{el}^{*}p_{el}), \tag{1}$$

where S_{el} is the elemental area, $\Re$ denotes the real part, and $*$ denotes conjugation.

The total power, W, radiated by the panel can then be calculated by defining vectors $\mathbf{v}$ and $\mathbf{p}$ whose elements are the velocities and pressures of each element and the total power output can be written as

$$w = \left(\frac{S_{el}}{2}\right)\Re(\mathbf{v}^{H}\mathbf{p}). \tag{2}$$

The pressure at each elemental position can also be expressed as a function of the velocity of each of the elemental sources

$$\mathbf{p} = \mathbf{Z}\mathbf{v}, \tag{3}$$

where $\mathbf{Z}$ is a matrix of acoustic transfer impedances which relates the pressure at each element to the velocity at each element and, the total acoustic power radiated is thus

$$W = \left(\frac{S_{el}}{2}\right)\Re(\mathbf{v}^{H}\mathbf{Z}\mathbf{v}) = \mathbf{v}^{H}\mathbf{R}\mathbf{v}, \tag{4}$$

where

$$\mathbf{R} = \left(\frac{S_{el}}{2}\right)\Re(\mathbf{Z}) \tag{5}$$

and the symmetry of $\mathbf{Z}$ due to reciprocity has been used.

The specific acoustic transfer impedance between elements i and j (which is the i,jth element of $\mathbf{Z}$) is given by [9, 20]

$$Z_{ij} = \frac{\mathrm{j}\omega\rho_0 S_{el}}{2\pi r_{ij}} \mathrm{e}^{-\mathrm{j}kr_{ij}}, \tag{6}$$

where r_{ij} is the distance between elements i and j. This equation is derived from the equation for radiation from a baffled, pulsating half-sphere [9]. The elements of $\mathbf{R}$ are then given by

$$R_{ij} = \frac{\omega^2\rho_0 S_{el}^2}{4\pi c_0}\left[\frac{\sin(kr_{ij})}{kr_{ij}}\right], \tag{7}$$

so that

$$\mathbf{R} = \frac{\omega^2\rho_0 S_{el}^2}{4\pi c_0}\begin{bmatrix} 1 & \dfrac{\sin kr_{12}}{kr_{12}} & \cdots & \dfrac{\sin kr_{1I}}{kr_{1I}} \\ \dfrac{\sin kr_{21}}{kr_{21}} & 1 & \cdots & \cdots \\ \cdots & \cdots & \cdots & \cdots \\ \dfrac{\sin kr_{I1}}{kr_{I1}} & \cdots & \cdots & 1 \end{bmatrix}. \tag{8}$$

The matrix $\mathbf{R}$ is seen to be symmetric (due to reciprocity), real (proportional to $\Re(\mathbf{Z})$), and positive definite (as the power output of the plate must be greater than zero unless velocity is zero). This means that it can be decomposed into a set of orthogonal real eigenvectors with positive real eigenvalues:

$$\mathbf{R} = \mathbf{Q}^{\mathrm{T}}\mathbf{\Lambda}\mathbf{Q}, \tag{9}$$

where $\mathbf{Q}^{\mathrm{T}}$ is a real and unitary matrix of orthogonal eigenvectors, and $\mathbf{\Lambda}$ is a diagonal matrix whose elements λ_i are the eigenvalues and are positive real numbers.

If this eigenvector/eigenvalue decomposition (equation (9)) is substituted into the equation representing radiated power for the elemental radiator approach, equation (4) one obtains

$$W = \mathbf{v}^H\mathbf{R}\mathbf{v} = \mathbf{v}^H\mathbf{Q}^{\mathrm{T}}\mathbf{\Lambda}\mathbf{Q}\mathbf{v}. \tag{10}$$

Now define $\mathbf{y} = \mathbf{Q}\mathbf{v}$, as the vector of radiation mode amplitudes, in terms of the velocities of individual elements, so that

$$W = \mathbf{y}^H\mathbf{\Lambda}\mathbf{y} = \sum_{i=1}^{I} \lambda_i |y_i|^2, \tag{11}$$

where the final form follows from the fact that $\mathbf{\Lambda}$ is diagonal.

The power output due to any one of these eigenvectors is then equal to its amplitude squared multiplied by its corresponding eigenvalue. This equation also shows that the modes are radiating independently since there are no off-diagonal terms in the matrix $\mathbf{\Lambda}$. The total radiated sound power can thus be calculated as a sum of individual mode amplitudes squared multiplied by their corresponding eigenvalues.

Figure 1 shows the radiation efficiencies of the first few radiation modes as a function of non-dimensional frequency obtained by the eigenvalue/eigenvector decomposition of $\mathbf{R}$. It is clear that, at low frequencies, the radiation efficiency of the first radiation mode is very large in comparison with the efficiencies of the other modes, which would suggest that controlling this radiation mode would be a good strategy. Figure 2 shows the shapes of the first six radiation modes at a low non-dimensional frequency of 0·5. The first radiation

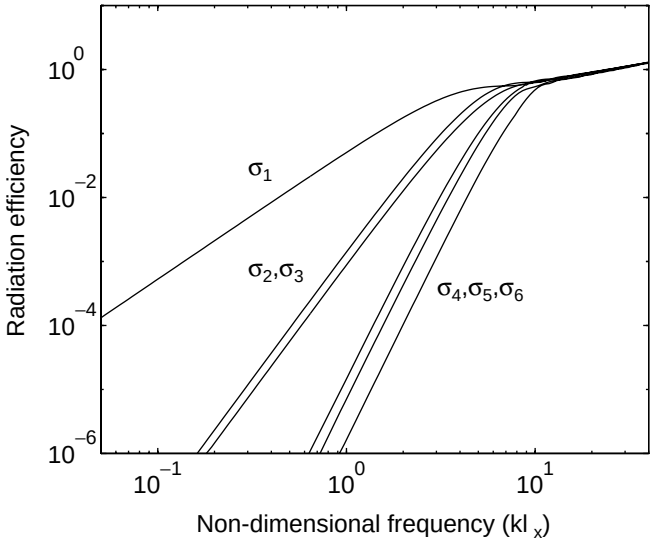

Figure 1. Radiation efficiencies of low order radiation modes.

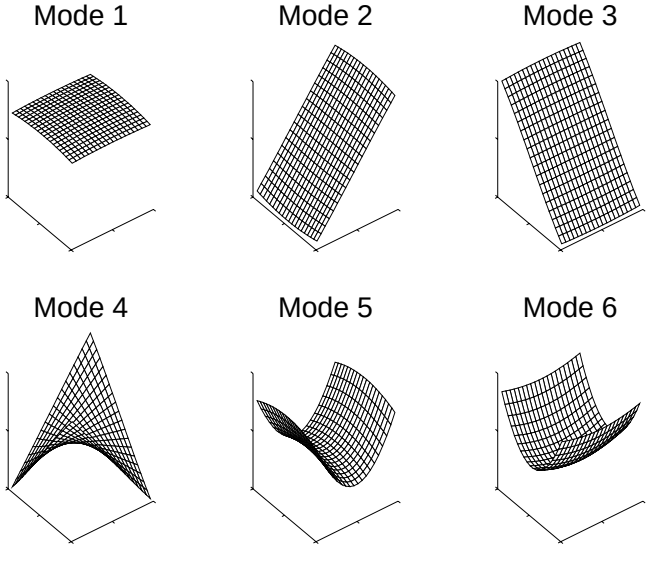

Figure 2. Shapes of first six radiation modes at a non-dimensional frequency of 0·5.

mode shows each element of the plate vibrating with almost the same phase and amplitude, and thus its amplitude is proportional to the volume velocity of the plate. The shape of the first radiation mode, obtained from the eigenvectors of **R**, at non-dimensional frequencies of 0·5 and 5 are shown in Figure 3. There is a clear difference in the shape over this frequency range. The changing shape of the first radiation mode with frequency will be considered below.

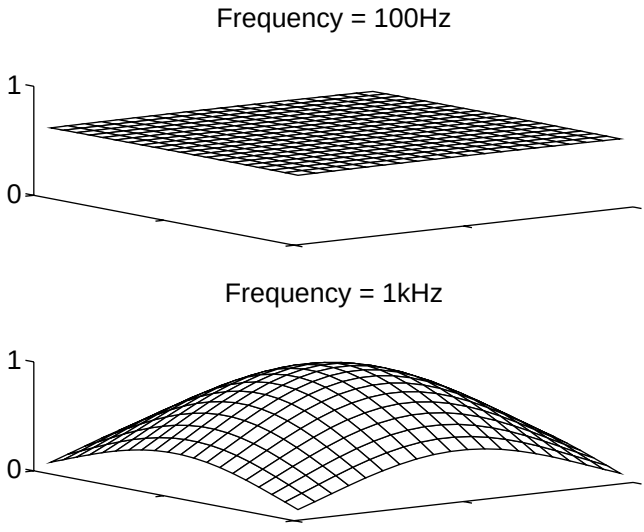

Figure 3. Shape of first radiation mode at non-dimensional frequencies of 0·5 and 5 (normalized amplitudes).

The important conclusions from Figures 1 and 2 are that radiation modes are found to have a number of advantages when it comes to active structural acoustic control such as the following:

(1) They radiate sound independently.
(2) The first radiation mode is seen to have a much larger radiation efficiency than the other radiation modes at low frequencies.
(3) The shape of this first radiation mode is found to have a very simple form. At very low frequencies, it corresponds to the volume velocity of the plate.

These provide the motivation for looking at the control of volume velocity during the rest of this paper; by reducing the volume velocity, the total radiated power should also be reduced.

3. APPROXIMATION TO VOLUME VELOCITY USING MULTIPLE ACCELEROMETERS

Consider a plate whose co-ordinate system is shown in Figure 4. The lengths of the sides in the x and y directions are given by l_x and l_y, respectively. Movement in the direction of the z-axis is denoted by w and only this form of vibration will be considered here since it is the out-of-plane vibration which gives rise to sound radiation.

The plate is considered to be excited by an incident plane wave with angle of incidence $\theta = \phi = 45^\circ$ which is chosen to excite all structural modes. This incident plane waves act as the primary disturbance and, assuming the plate is simply supported around its edges and light fluid loading, the resulting plate excitation and resulting sound radiation can be calculated analytically as shown by Roussos [21]. The properties of the modelled plate used are shown in Table 1 and the modelling techniques are described in more detail in reference [22].

The secondary control force is generated on the plate by means of a 25 mm by 25 mm piezoceramic patch placed at the centre of the plate. Although there are a number of

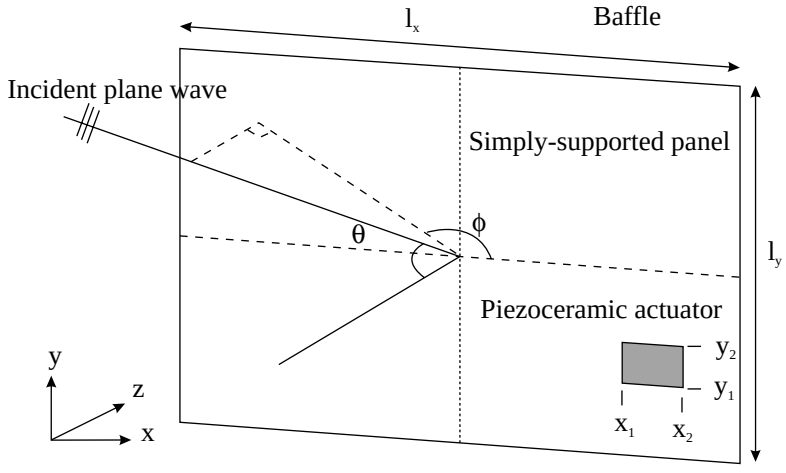

Figure 4. Co-ordinate system of a thin rectangular plate.

TABLE 1

Material properties of plate

Property	Value
Length (x direction)	0.278 m
Length (y direction)	0.247 m
Thickness	1 mm
Young's modulus	71×10^9 N m^3
The Poisson ratio	0·33
Density	2720 Kg/m^3
Damping ratio	0·2%
Unity non-dimensional frequency (i.e., when $kl_x = 1$)	195 Hz

possible options for structural actuators, piezoceramic actuators currently seem to be the most suitable due to their low cost, light weight, and the fact that they can be shaped easily and are easy to incorporate into the structure to be controlled. They can also deliver relatively large forces to the structure under control with a low current, high voltage supply. References which discuss the theory and use of piezoceramic actuators include [7, 23]. The mass loading and damping effects of the piezoceramic actuator are assumed to be negligible and so the sound power transmitted through the plate with no control is unaffected by the actuator's presence. Placement of the actuators and sensors is another important issue which has a large effect on the performance of control systems and a number of techniques exist for their optimal placement. Many optimization techniques exist as outlined in reference [24] for example. A more intuitive method based on physical arguments is given by Sors and Elliott [25]. A single actuator is used here for simplicity, but as this is placed in the middle of the plate, it is able to control the odd–odd volumetric modes with maximum effect and so this seems a reasonable position for the actuator.

Single frequency feedforward simulations, which give the best performance that can be achieved using a given physical system, are used in which the amplitude and phase of the

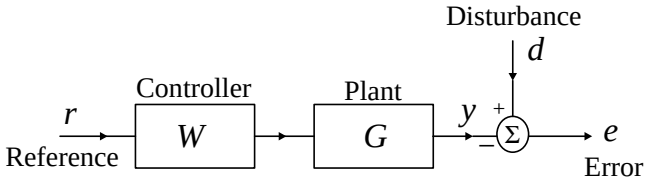

Figure 5. Block diagram of feedforward control.

control signal are calculated from signals measured by some form of structural sensor. In practice, a reference signal would be required. The block diagram for the feedforward simulations is shown in Figure 5. In the diagram, G represents the plant, i.e., the frequency response function between the input to the secondary actuator and the output from the error sensor, and W represents the feedforward controller.

Two different types of sensor are used. In the first case, the total radiated power will be minimized. In practice, this method would require the use of a large number of error microphones in the far field. This is often impractical and so error sensors bonded directly to the structure are used in the second control strategy which minimizes the output of such an error sensor either in the form of summed accelerometer outputs or, a distributed volume velocity sensor. The aim is to get as close to the ideal control, given by the minimum radiated power, as possible.

For the first control strategy of controlling radiated sound power, the complex velocity distribution of the plate due to tonal excitation can be expressed as a combination of velocities due to primary (disturbance) and secondary (control) forces. Furthermore, the velocity distribution due to secondary actuators can be expressed as the velocity vector due to a unit input voltage, $\mathbf{g}$, multiplied by a complex control signal u, such that

$$\mathbf{v} = \mathbf{v}_p + \mathbf{g}u, \tag{12}$$

where $\mathbf{v}_p$ is the velocity distribution due to the primary incident wave.

By substituting this into the equation for sound radiation, (4), it can be rearranged into the well-known Hermitian quadratic form,

$$W = u^* A u + u^* b + b^* u + c, \tag{13}$$

where

$$A = \mathbf{g}^h \mathbf{R} \mathbf{g}, \qquad b = \mathbf{g}^H \mathbf{R} \mathbf{v}_p, \qquad c = \mathbf{v}_p^{\mathrm{T}} \mathbf{R} \mathbf{v}_p, \tag{14}$$

which is minimized by using the complex control voltage, u_m, given by

$$u_m = -A^{-1} b. \tag{15}$$

The second control strategy focuses on the cancellation of the error sensor output and can be calculated in a way similar to that above. The aim is to cancel the total charge output of the sensors attached to the panel. The charge output can be written as a combination of contributions from primary and secondary sources:

$$q_{\mathrm{tot}} = q_p + q_h u, \tag{16}$$

where q_h, is the charge output due to a unit input voltage to the actuator. To set q_{tot} to zero, the control voltage is

$$u_e = -\frac{q_p}{q_h}. \tag{17}$$

As the excitation of the plate is assumed to be tonal, with a known frequency, the control problem reduces to adjustment of the amplitude and phase of the complex control input, u, at that frequency. In each simulation, the following curves are shown:

(1) The power transmission ratio before control as defined by

$$T = \frac{W_r}{W_i}, \tag{18}$$

where W_r is the sound power radiated by the panel and the incident acoustic power is defined by Roussos [21] to be

$$W_i = \frac{|P_i^2| l_x l_y \cos(\theta)}{2\rho_0 c_0}. \tag{19}$$

(2) The power transmission ratio after the input to the actuator has been adjusted at each frequency to minimize the radiated sound power.
(3) The power transmission ratio after the input to the actuator has been adjusted at each frequency to cancel the sensor output whether that is provided by the sum of accelerometer outputs or by a volume velocity sensor.

The first control simulations shown in Figure 6 compare the control of radiated sound power, equation (15), with the control of true volume velocity, equation (17), using the single centrally placed actuator.

At all frequencies the ideal control curve, obtained by minimizing sound radiation, is lower than the curve which is obtained by minimizing the volume velocity as expected. This is the reference curve which shows the best possible attenuation which can be achieved using the given transducer configuration. The total attenuation over the 1 kHz frequency range is 7·9 dB, but at any single frequency can be very large. The value for overall attenuation is weighted towards high frequencies where the overall sound power radiation is increased. However, this is the frequency region with the lowest attenuation,

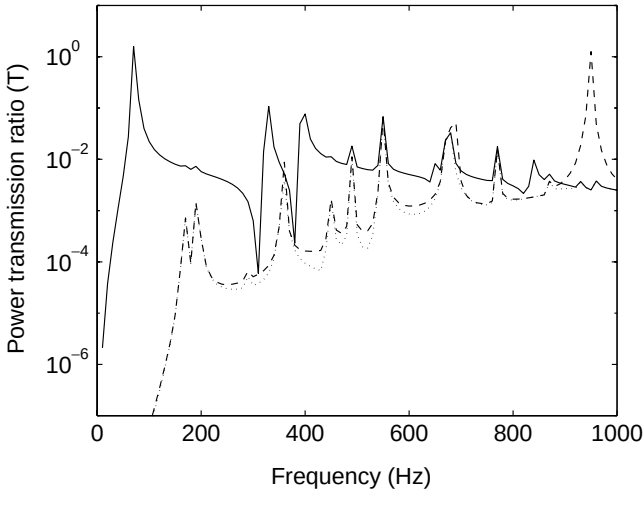

Figure 6. Power transmission ratio before control (solid), using feedforward control of sound power (dotted) and, using feedforward control of volume velocity (dashed).

so the value of overall attenuation does not give a good indication of the control performance at low frequencies.

As there are practical problems associated with the sensors for both of these control strategies outlined in the introduction, the remainder of this paper considers the use of accelerometers and in particular, using increasing numbers of accelerometers with their outputs summed to give an estimate to the true volume velocity. The feedforward algorithm given by equation (17) is used to calculate the control voltage where the output signal is given by the sum of the accelerometer outputs. Results are presented in terms of the performance of the various sensor configurations rather than by comparing the sensor output signals.

The results of cancelling the summed output of different numbers of accelerometers, as an estimate of the volume velocity are shown in Figure 7. Each subfigure shows the configuration of piezoceramic actuators and accelerometers, although the x and y dimensions of the plate are not to scale, and shows four curves; the power transmission ratio before control (solid), using control of radiated sound power (dotted), using control of true volume velocity (dashed), and using control of the summed accelerometer outputs (dash-dotted). Forty-nine structural modes were used in the theoretical model of the plate, with natural frequencies up to 3527 Hz. The number of elements in the grid was around 20×20, but was varied slightly depending on the number of accelerometers such that they were all positioned at centres of elements. The results for the control of radiated power and the control of volume velocity with a single piezoceramic actuator remain constant in

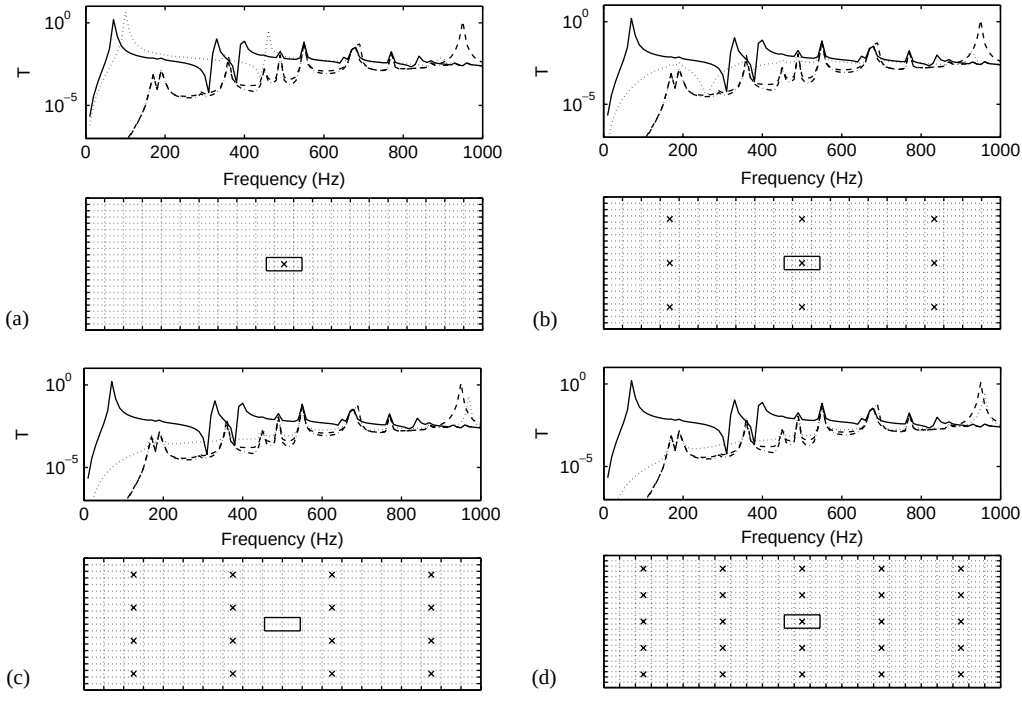

Figure 7. Results of SISO simulations of active feedforward control showing power transmission ratio, T, of radiated sound power to incident sound power for plane wave excitation at $\theta = \phi = 45^\circ$ (con't): a single actuator is used to cancel the summed output from a number of accelerometers or true volume velocity or radiated power. Solid line is power transmission ratio before control, dotted line is after control of radiated power, dashed line is after control of volume velocity and thick dash–dot line is after control of summed accelerometer output.

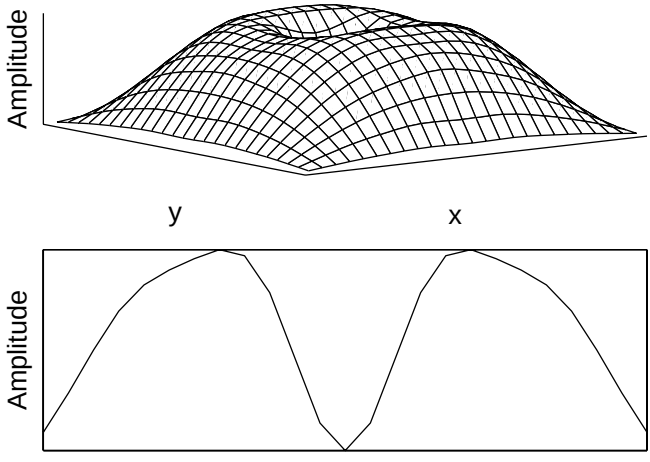

Figure 8. First structural mode after control using a single piezoceramic actuator and single accelerometer: (a) Whole plate, (b) section through mid-plane of plate.

Figures 7(a)–7(d), as these two strategies depend only on the actuator configuration which remains the same. The aim of these figures is to see whether, by increasing the number of accelerometers, a good estimate of the volume velocity can be obtained.

The first comparison between sensors in Figure 7(a) shows the control of the output of one accelerometer with the control of true volume velocity or control of sound power. Figure 8 shows the vibration distribution of the plate after control of a pure tonal disturbance at 72 Hz, the natural frequency of the $(1, 1)$ mode of the plate, using a piezoceramic patch actuator with a centrally placed accelerometer. Before control, the vibration of the plate takes a sinusoidal form. The effect of the actuator cancelling the output of the accelerometer, as shown in the figure, is to pin that part of the plate. The dynamics of the plate are thus changed and the structure displays a new frequency response function with a new set of resonances. The effect is that the radiated sound power is not controlled even though the kinetic energy and vibrational levels may be reduced. This demonstrates the difference between ASAC and ACV.

The extra resonance at 100 Hz is suppressed when the sum of the outputs of nine accelerometers is controlled in Figure 7(b). With the use of 16 or 25 accelerometers, Figure 7(c) or 7(d), it becomes clear that a variable similar to the volume velocity is being controlled. The graphs show that at low frequencies, the control of volume velocity is still working slightly better. At high frequencies, there is somewhat less amplification when using the accelerometers. This amplification effect is known as spillover and is described below.

Table 2 gives values of attenuation averaged over a 0–500 Hz frequency range, which is where the best control performance is achieved. It is evident from examining Figure 7 that large reductions in radiated sound power can be achieved at low frequencies and that at high frequencies, there may even be some increase in the radiated power, i.e., spillover. Spillover can occur when the secondary source is unable to efficiently drive the first radiation mode. If the secondary source has to drive extremely hard to cancel the volume velocity of the plate, other higher order radiation modes may begin to radiate significant amounts of sound power. At high frequencies, where the volume velocity is no longer a good approximation to the shape of the first radiation mode, other radiation modes can

TABLE 2

Table of attenuations in sound power over a 500 Hz *bandwidth for different control strategies and different arrangements of accelerometers used in the estimate of volume velocity*

Sensor	Attenuation in transmitted sound power (dB)
Sound power	20·2
True volume velocity	19·1
Volume velocity estimated with	
1	− 3·8
9	14·0
16	18·1
25	18·3
400	19·1

also be excited by the secondary actuator. This is shown, for example, by an increase in the power transmission ratio at around 950 Hz for the control of volume velocity. However, the low frequency region is the region of most interest in active control applications.

Figure 9 shows the attenuation in radiated sound power as a function of the number of accelerometers for a plane wave incident with angles $\theta = \phi = 45^\circ$ averaged over a 500 Hz frequency range. It is evident that by increasing the number of accelerometers, the attenuation tends to the use of a true volume velocity sensor. In the limit, where the number of accelerometers is equal to the number of elements used in the plate model, the attenuations for the two methods are the same. The configuration using 16 accelerometers strikes a good and practical balance between obtaining a good estimate of the volume velocity and the number of accelerometers required.

An analytical estimate of the number of accelerometers required to give a reasonable practical estimate of volume velocity can be obtained by calculating the number of structural modes with natural frequencies below the frequency for which the radiation efficiency of all the radiation modes becomes similar. Below this frequency, only the first radiation mode needs to be considered. Figure 1 shows that the radiation efficiencies of the radiation modes become similar at around $kl_x = 10$, which thus sets the upper frequency limit for which volume velocity control alone can be used, and Figure 10 shows that for the plate considered above, the number of structural modes with a natural frequency below $kl_x = 10$ is in the region of 20–25. In order to estimate the volume velocity, approximately this number of accelerometers are required, which explains why around 16–25 is a good estimate for the number of required accelerometers to estimate volume velocity in this case.

In general, the number of modes with natural frequencies below ω for a flat homogeneous plate of dimensions l_x, l_y, mass per unit area m, and bending stiffness D is approximately [26]

$$N(\omega) = \frac{l_x l_y}{4\pi}\sqrt{\frac{m}{D}}\,\omega. \tag{20}$$

If the number of accelerometers is equal to the number of modes when $kl_x = 10$, i.e., $\omega = 10c_0/l_x$, where c_0 is the speed of sound, then the required number of accelerometers is

$$N = \frac{5}{3\pi}\,c_0 l_y\sqrt{\frac{m}{D}}. \tag{21}$$

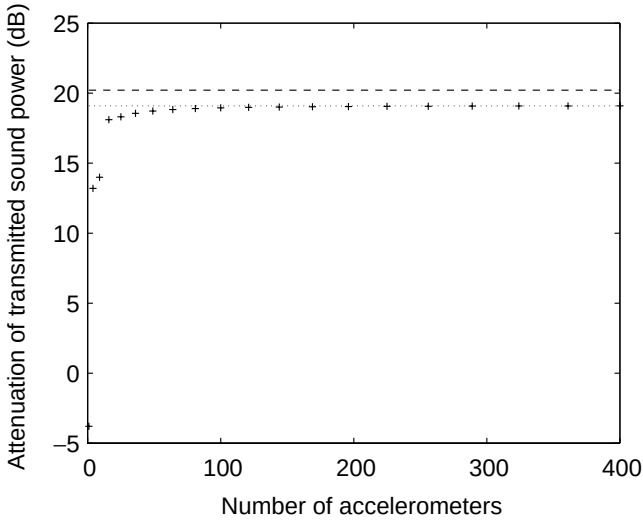

Figure 9. Attenuation in sound power radiated as a function of number of accelerometers for a feedforward active control system using a single central piezoceramic patch actuator to cancel the summed output of increasing numbers of accelerometers. Dashed line represents control of radiated power, dotted line represents control of volume velocity, averaged over 500 Hz.

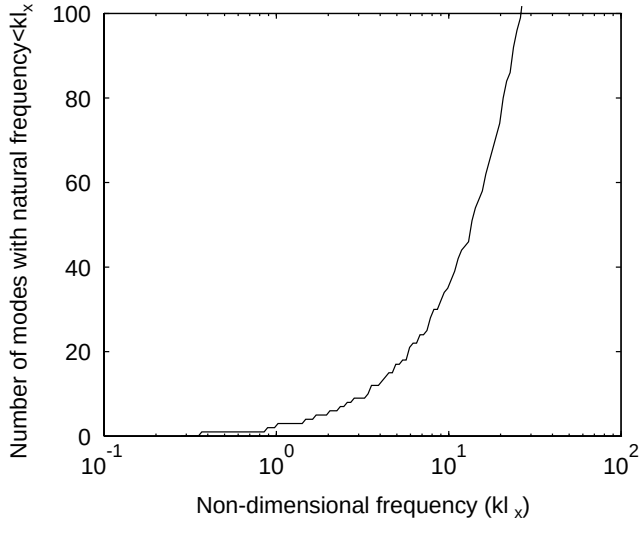

Figure 10. Number of structural modes with natural frequency under a given frequency for the simply supported plate considered above.

For the plate used in this paper, this equation predicts that around 29 accelerometers would be required.

4. OTHER COST FUNCTIONS USING MULTIPLE ACCELEROMETERS

In the previous section, a number of accelerometers were placed on a plate and their outputs were combined by a simple summation to obtain a reference signal which was fed

to a controller. Using these accelerometers, it is natural to investigate different ways of combining the outputs of the accelerometers to obtain other reference signals which may lead to a good reduction in the radiated power and, three of these cost functions are outlined below:

(1) Using the accelerometers to control high order, frequency-independent, radiation mode shapes.
(2) Controlling the frequency-dependent shape of the first radiation mode as opposed to the volume velocity.
(3) Using multiple single channel control systems on the plate.

4.1. CONTROL OF HIGH ORDER RADIATION MODES

Table 3 gives the additional reductions in sound power radiation up to 1 kHZ obtained when the sum of the squared amplitudes of higher order radiation modes are controlled by a feedforward control system with a single centrally placed piezoceramic actuator. These can be calculated easily using equation (11), where the eigenvalue λ_i can be found from the relevant term in the decomposition of the matrix **R** (see equation (8)) and gives the power radiated by the corresponding radiation mode in Figure 2. The small values indicate that, at the frequencies considered, it is far more important to control the first radiation mode as well as possible than to consider higher order radiation modes.

4.2. CONTROL OF FREQUENCY-DEPENDENT SHAPE OF FIRST RADIATION MODE

This strategy examines controlling the frequency-dependent shape of the first radiation mode instead of the volume velocity, which is only a good approximation to the shape of the first radiation mode at low frequencies. The shape was seen to change significantly over a 1 kHz frequency range in Figure 3. The following analysis deals with how the multiple accelerometers can best be used to control the first radiation mode in practice and relies on the fact that the radiation mode shapes can be obtained from the eigenvalue/eigenvector decomposition of the matrix **R**. The position of each accelerometer for a given radiation mode at a given frequency can then be calculated and stored in a frequency-dependent weighting for the accelerometer instead of using a weighting of unity for each

TABLE 3

Reduction in the average power radiated below 1 kHz *when different numbers of radiation modes are controlled*

Radiation mode	Additional reduction in sound power (dB)
1	11·3
2	0·1
3	0·1
4	$<0{\cdot}1$
5	$<0{\cdot}1$
6	$<0{\cdot}1$
7	$<0{\cdot}1$

accelerometer, which would be equivalent to minimizing the approximation to the volume velocity.

As an example, consider an arrangement with four accelerometers used to calculate the amplitude of the first radiation mode y_1—the weightings for each of the accelerometers at each frequency can be found from the relevant elements of the first eigenfunction of **R**:

$$y_1(\omega) = \tfrac{1}{4}(Q_1(\omega)v_1 + Q_2(\omega)v_2 + Q_3(\omega)v_3 + Q_4(\omega)v_4), \tag{22}$$

where $Q_1(\omega)$ refers to the element of the first eigenfunction of **R** corresponding to the position of the first accelerometer, v_1 corresponds to the velocity at the point of the first accelerometer, etc. These are similar to the radiation filters used by Bauman *et al.* [27].

A comparison of the control of volume velocity, an approximation to the volume velocity using 16 accelerometers, and an approximation to the first radiation mode using 16 accelerometers, is shown in Figure 11. Controlling an approximation to the first radiation mode using the 16 accelerometers rather than an approximation to the volume velocity itself using 16 accelerometers is seen to give some performance increase in the mid-frequency range, particularly at frequencies away from resonances.

4.3. MULTIPLE SINGLE CHANNEL CONTROL SYSTEMS

Another possible configuration currently being investigated would include a number of single channel control systems on the plate each with its own piezoceramic actuator, collocated accelerometer and a simple velocity feedback controller for example. Each of these local control systems could be used independently. This type of configuration could be implemented easily using microelectromechanical systems (MEMS) which is currently an area of rapid development [28]. Recent work [29] suggests that this technique may have additional advantages for vibration control.

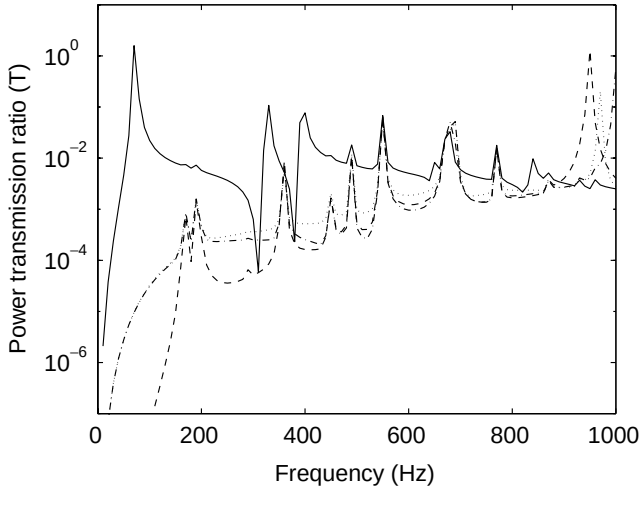

Figure 11. Simulations of feedforward control in which a single actuator is used to minimize the output of either a true volume velocity sensor (dashed line), summed output of 16 accelerometers, i.e., approximation to volume velocity (dotted line), or approximation to first radiation mode using 16 accelerometers (dash-dotted line).

5. CONCLUSIONS

This paper has considered a number of ways in which multiple accelerometers on a plate could be used to obtain cost functions for ASAC. The main focus has been on summing the outputs from increasing numbers of accelerometers to give a signal which is an approximation to the volume velocity of the plate.

In the first section of the paper, the theory of radiation modes is reviewed and the reasons for trying to control the volume velocity of the plate are outlined. Previous attempts at this have used a quadratically shaped PVDF film to obtain the volume velocity, but as this results in a strain sensor, it has the disadvantage of not being able to measure whole-body motion. In this paper, the integrated output from an array of accelerometers were used instead which have the additional advantage of allowing multi-channel control.

Summing the outputs of increasing numbers of accelerometers was found to tend to the use of a volume velocity sensor and, by reducing the amount of spillover at high frequencies, certain numbers of accelerometers were found to work particularly well for the plate used in the simulations. The reasons were explained in terms of the number of significantly radiating structural modes.

In a final section, some multi-channel configurations were examined in which the outputs of the accelerometers were used in some other way than a simple summation. The advantages relative to the control of volume velocity were found to be small confirming the effectiveness of this simple control strategy.

An experimental rig has been built following the simulations outlined in this paper and it is hoped that feedback control will be possible in the near future using accelerometers as sensors.

ACKNOWLEDGMENTS

This work has been sponsored by the TNO Institute of Applied Physics, Delft, The Netherlands.

REFERENCES

1. C. R. Fuller 1988 in *Proceedings of Inter-Noise*' 88, *Avignon*, *France*, 1061–1064. Analysis of active control of sound radiation from elastic plates by force inputs.
2. L. Meirovitch and M. A. Norris 1984 in *Proceedings of Inter-Noise*' 84, *Honolulu*, *U.S.A.*, 477–482. Vibration control.
3. C. R. Fuller 1990 *Journal of Sound and Vibration* **136**, 1–15. Active control of sound transmission/radiation from elastic plates by vibration inputs. I: analysis.
4. B. Wang 1991 *Journal of the Acoustical Society of America* **90**, 2820–2830. Active control of noise transmission through rectangular plates using multiple piezoelectric or point force actuators.
5. E. K. Dimitriadis, C. R. Fuller and C. A. Rogers 1991 *Journal of Vibration and Acoustics. Transactions of the American Society of Mechanical Engineers* **113**, 100–107. Piezoelectric actuators for distributed vibration excitation of thin plates.
6. E. K. Dimitriadis and C. R. Fuller 1991 *American Institute of Aeronautics and Astronautics Journal* **29**, 1771–1777. Active control of sound transmission through elastic plates using piezoelectric actuators.
7. C. A. Fuller, S. J. Elliott and P. A. Nelson 1996 *Active Control of Vibration*. London: Academic Press.
8. C. R. Fuller, C. A. Rogers and H. H. Robertshaw 1992 *Journal of Sound and Vibration* **57**, 19–39. Control of sound radiation with active/adaptive structures.

9. M. E. JOHNSON 1996 *Ph.D. Thesis*, *Institute of Sound and Vibration Research*, *University of Southampton*. Active control of sound transmission.
10. A. PREUMONT 1997 *Vibration Control of Active Structures. An Introduction*. The Netherlands: Kluwer Academic Publishers.
11. M. E. JOHNSON and S. J. ELLIOTT 1995 *Journal of the Acoustical Society of America* **94**, 2174–2186. Active control of sound radiation using volume velocity cancellation.
12. S. J. ELLIOTT and M. E. JOHNSON 1993 *Journal of the Acoustical Society of America* **94**, 2194–2204. Radiation modes and the active control of sound power.
13. J. REX and S. J. ELLIOTT 1992 in *Proceedings of the First International Conference on Motion and Vibration Control*, *Yokohama*, *Japan*, 339–343. The QWSIS—a new sensor for structural radiation control.
14. M. E. JOHNSON, T. SORS, S. J. ELLIOTT and B. RAFAELY 1997 in *Proceedings of Active*' 97, *Budapest*, *Hungary*, 1007–1020. Feedback control of broadband sound radiation using a volume velocity sensor.
15. J. P. MAILLARD and C. R. FULLER 1997 in *Proceedings of Active*' 97, *Budapest*, *Hungary*, 1021–1034. Active control of sound radiation from cylinders with piezo-electric actuators and structural acoustic sensing.
16. J. P. MAILLARD and C. R. FULLER 1994 *Journal of the Acoustical Society of America* **95**, 3252–3261. Advanced time domain wave-number sensing for structural acoustic systems. I: theory and design.
17. J. P. MAILLARD and C. R. FULLER 1994 *Journal of the Acoustical Society of America* **95**, 3262–3272. Advanced time domain wave-number sensing for structural acoustic systems. II: active radiation control of a simply supported beam.
18. J. P. MAILLARD and C. R. FULLER 1995 *Journal of the Acoustical Society of America* **98**, 2613–2621. Advanced time domain wave-number sensing for structural acoustic systems. III: experiments on active broadband radiation control of a simply-supported plate.
19. A. PREUMONT, A. FRANCOIS and S. DUBRU 1999 *Journal of Vibration and Acoustics*, *Transactions of American Society of Mechanical Engineers* **21**, 446–452. Piezoelectric array sensing for real-time, broad-band sound radiation measurement.
20. P. VITIELLO, P. A. NELSON and M. PETYT 1989 *ISVR Technical Report No*. 183. Numerical studies of the active control of sound transmission through double partitions.
21. L. A. ROUSSOS 1985 *Technical Report NASA-TP*-2398, *NASA*. Noise transmission loss of a rectangular plate in an infinite baffle.
22. T. C. SORS 2000 *Ph.D. Thesis*, *Institute of Sound and Vibration Research*, *University of Southampton*. Active structural acoustic control of sound transmission through a plate.
23. C. K. LEE 1990 *Journal of the Acoustical Society of America* **87**, 1144–1158. Theory of laminated piezoelectric plates for design of distributed sensors/actuators. Part I: governing equations and reciprocal relationships.
24. S. ELLIOTT 2001 *Signal Processing for Active Control*. U.K.: Academic Press.
25. T. C. SORS and S. J. ELLIOTT 1999 *Journal of Smart Materials and Structures* **8**, 301–314. Modelling and feedback control of sound radiation from a vibrating panel.
26. R. G. WHITE and J. G. WALKER (editors). 1982 *Noise and Vibration*. Great Britain: Ellis Horwood.
27. W. T. BAUMANN, W. R. SAUNDERS and H. R. ROBERTSHAW 1991 *Journal of the Acoustical Society of America* **90**, 3202–3208. Active suppression of acoustic radiation from impulsively excited structures.
28. H. SUBRAMANIAN, V. K. VARADAN, V. V. VARADAN and M. J. VELLEKOOP 1997 *Journal of Smart Materials and Structures* **6**, 730–738. Design and fabrication of wireless remotely readable MEMS based microaccelerometers.
29. S. J. ELLIOTT, P. GARDONIO, T. C. SORS and M. BRENNAN 2001 *Proceedings of the SPIE Eighth Annual International Symposium on Smart Materials and Structures, San Diego, CA, USA*. Active vibro-acoustic control with multiple local feedback loops.